Experimental studies of the defect structure of the TiO2(110) surface before and after the exposure to oxygen, hydrogen and carbon monoxide

by Gerd Heinrich Rocker

A thesis submitted in partial fulfillment of the requirements for the degree of Doctor of Philosophy in Physics

Montana State University

Abstract:
The electronic defect structure of Ti02 (110) before and after exposure to O2, H2 and CO was studied by means of XPS, XAES., AES, EELS, ELS and conductivity as well as work function changes. Surface defects, created by high temperature treatment, ion bombardment and by evaporating submonolayer amounts of Ti, lead to an additional peak in the TiLMV Auger signal, changes in the valence band structure and broadening and/or additional peaks in the Ti2p, Ti3p and 01s core-levels. These effects result from the formation of Ti3+ in a Ti-V0-Ti complex at the surface and induce an increase in the surface conductivity as well as more (less) pronounced conductivity changes upon the adsorption of 02 (H2 and CO), if compared to the stoichiometric surface. In the presence of defects the adsorption of any of these gases also results in an increase of the work function whereas a decrease (increase) was observed during H2 and CO (02) exposure to ideal surfaces. The results are discussed quantitatively in terms of a modified charge transfer model.

EXPERIMENTAL STUDIES OF THE DEFECT STRUCTURE OF THE TiO_2(110) SURFACE BEFORE AND AFTER THE EXPOSURE TO OXYGEN, HYDROGEN AND CARBON MONOXIDE

by

Gerd Heinrich Rocker

A thesis submitted in partial fulfillment
of the requirements for the degree

of

Doctor of Philosophy

in

Physics

MONTANA STATE UNIVERSITY
Bozeman, Montana

August 1985

APPROVAL

of a thesis submitted by

Gerd Heinrich Rocker

This thesis has been read by each member of the thesis committee and has been found to be satisfactory regarding content, English usage, format, citations, bibliographic style, and consistency, and is ready for submission to the College of Graduate Studies.

8-5-85
Date

John Hermanson
Co-chairperson,
Graduate Committee

Approved for the Major Department

8-5-85
Date

Robert Stevens
Head, Major Department

Approved for the College of Graduate Studies

9-8-85
Date

M B Malone
Graduate Dean

STATEMENT OF PERMISSION TO USE

In presenting this thesis in partial fulfillment of the requirements for a doctoral degree at Montana State University, I agree that the Library shall make it available to borrowers under rules of the Library. I further agree that copying of this thesis is allowable only for scholarly purposes, consistent with "fair use" as prescribed in the U.S. Copyright Law. Requests for extensive copying or reproduction of this thesis should be referred to University Microfilms International, 300 North Zeeb Road, Ann Arbor, Michigan 48106, to whom I have granted "the exclusive right to reproduce and distribute copies of the dissertation in and from microfilm and the right to reproduce and distribute by abstract in any format."

Signature Gerd Rosse

Date 8/5/85

ACKNOWLEDGEMENTS

I would like to take this opportunity to thank my thesis advisor, Dr. Wolfgang Goepel, who suggested the research reported in this thesis. I am grateful to him for coming to Bozeman and giving valuable advice during numerous discussions. Also, I would like to express my sincere thanks to Dr. John Hermanson for his sustained support as the chairman of my Ph. D. committee during the absence of my thesis advisor. I deeply acknowlegde his helpful advice and the time he spent in reading the manuscript of this thesis. I am particularly grateful to Dr. James Anderson, who had the amazing ability to offer help and encouragement whenever physical problems arose and other advisors were unavailable. I greatly acknowlegde his valuable advice, his patience and his kind assistance during my measuring time in the CRISS lab. Special gratitude is extended to Dr. Gerald Lapeyre for awarding measuring time, and to Milton Jaehnig and Dr. David Frankel for their helpful support during numerous experiments. Furthermore, I deeply appreciate the technical assistance of Alfred Beldring. Without the electronic devices that he built, a major part of my experimental work would not have been possible. Finally, I gratefully acknowledge the generous financial support provided by an M. J. Murdock Charitable Trust Grant of Research Corporation.

TABLE OF CONTENTS

TABLE OF CONTENTS - CONTINUED

LIST OF TABLES

LIST OF FIGURES

LIST OF FIGURES - CONTINUED

LIST OF FIGURES - CONTINUED

LIST OF FIGURES - CONTINUED

Abstract

The electronic defect structure of TiO_2(110) before and after exposure to O_2, H_2 and CO was studied by means of XPS, XAES, AES, EELS, ELS and conductivity as well as work function changes. Surface defects, created by high temperature treatment, ion bombardment and by evaporating submonolayer amounts of Ti, lead to an additional peak in the TiLMV Auger signal, changes in the valence band structure and broadening and/or additional peaks in the Ti2p, Ti3p and O1s core-levels. These effects result from the formation of Ti^{3+} in a $Ti-V_O-Ti$ complex at the surface and induce an increase in the surface conductivity as well as more (less) pronounced conductivity changes upon the adsorption of O_2 (H_2 and CO), if compared to the stoichiometric surface. In the presence of defects the adsorption of any of these gases also results in an increase of the work function whereas a decrease (increase) was observed during H_2 and CO (O_2) exposure to ideal surfaces. The results are discussed quantitatively in terms of a modified charge transfer model.

CHAPTER 1

INTRODUCTION AND STATEMENT OF THE PROBLEM

Titanium dioxide is a transition-metal oxide and has proved its great practical importance in the field of gas sensors, catalysts, high-temperature-resistant semiconductors, masers, photodecomposition of water and the photo-oxidation of a number of organic and inorganic molecules (see chapter 2).

The underlying physical and chemical mechanisms, however, are not well understood yet. It is believed that surface point defects are responsible for the catalytic activity of titanium dioxide surfaces, in the sense that they provide adsorption sites for foreign gases and determine charge-transfer reaction rates (see chapter 2).

In this thesis, different methods for preparing stoichiometric and defective titanium dioxide surfaces will be presented. The interaction of various gases such as oxygen, hydrogen and carbon monoxide with these surfaces will be investigated by studying changes in the surface electronic structure. Measurements of changes in surface conductivity and work function as well as different electron spectroscopies will be applied as surface-sensitive experimental probes.

CHAPTER 2

LITERATURE SURVEY OF INVESTIGATIONS ON TITANIUM DIOXIDE

Bulk Properties and Bulk Defects

The three polymorphic structures of titanium dioxide (TiO_2) are known to be rutile, anatase and brookite [1,2,3]. The rutile structure to be investigated in this thesis is the most stable structure under atmospheric conditions at room temperature. It exhibits a tetragonal unit cell, which contains two titanium Ti^{4+} and four oxygen O^{2-} ions (Figure 1 and reference 4). Its coordination is 6:3 (oxygen-to-titanium neighbors).

The space group of the rutile structure is D_{4h}^{14}, whose irreducible representations, as well as those of its small groups, have been given by Dimmock and Wheeler and by Gay et al. [2,5,6].

Each titanium ion in the unit cell has two oxygen neighbors at a distance of 1.988 Å and four oxygen neighbors at a distance of 1.944 Å (Figure 1). Thus, each cation is surrounded by a nearly regular octahedron of six anions, and each anion is at the center of a nearly equilateral triangle of cations [2].

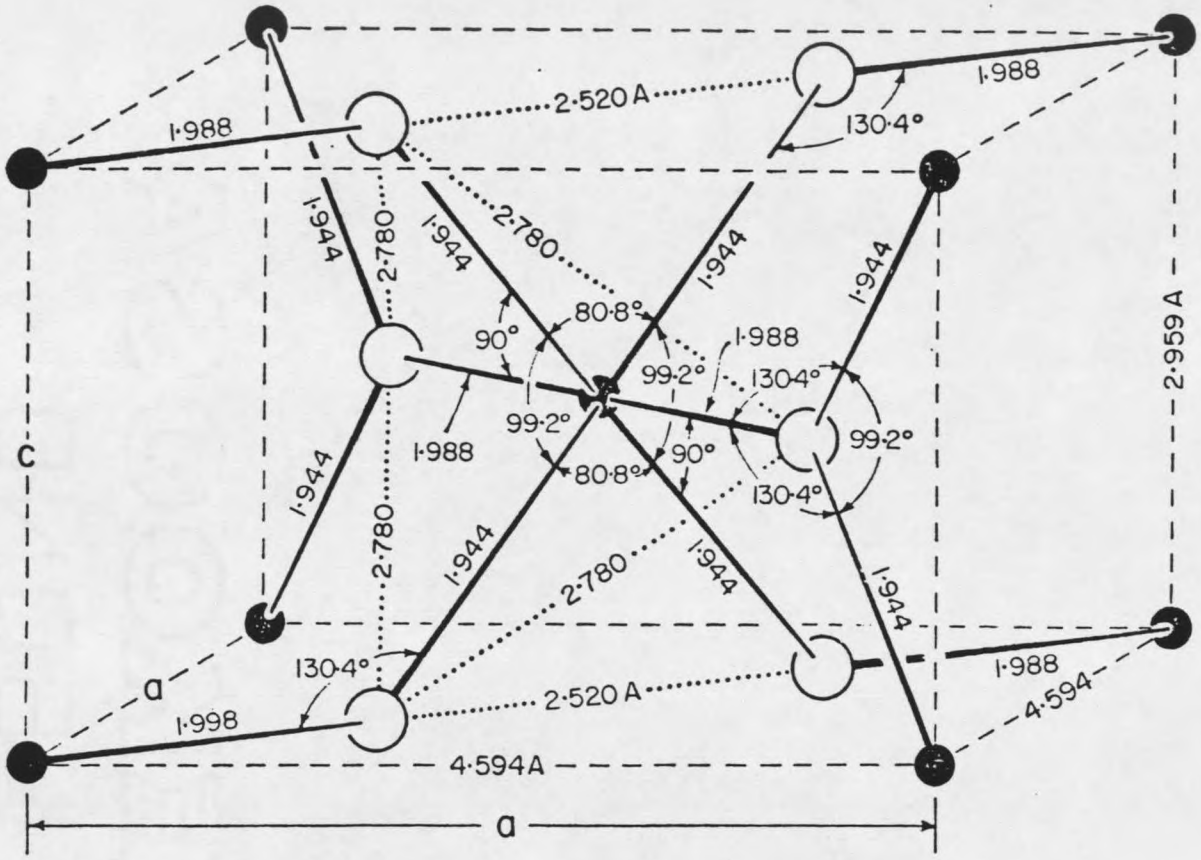

Figure 1. Unit cell of rutile TiO_2 (see reference 4). Black and white circles represent Ti^{4+} and O^{2-} ions, respectively.

From general group theoretical results [7] it is well-known that an octahedral ligand field causes the five degenerate Ti3d states to split into two states of e_g symmetry and three states of t_{2g} symmetry, but leaves the three O2p states unaffected. This effect is retrieved in the bulk electronic structure, since the octahedral environment is nearly preserved in the crystal, leading to two valence- and two conduction subbands of $e_g(3z^2-r^2,xy)$ and $t_{2g}(xz,yz,x^2-y^2)$ symmetry [2,8]. Due to the comparatively high ionicity of TiO_2 of 60-70 % [2] on Philip's ionicity scale, estimated from Raman Spectroscopy [9] and Positron Annihilation [10] studies, the valence and conduction bands are mainly derived from O2p and Ti3d orbitals, respectively. The fairly large optical band gap was determined to be 3.05 eV near room temperature [11]. The pure stoichiometric TiO_2 crystal is thus a transparent insulator showing a bulk conductivity of approximately $10^{-13}\,\Omega^{-1}cm^{-1}$ [12,13].

The phase diagram of the Ti-O system is complicated [14,15]. Below 2100 K (the melting point of TiO_2), there exists at least eight intermediate titanium oxides (Ti_nO_{2n-1}, n=3 to 10) between Ti_2O_3 (titanium sesquioxide) and TiO_2.

On reduction by heating in vacuum or hydrogen at 870 K for an hour, oxygen is partially lost from the TiO_2 lattice (the equilibrium oxygen partial pressure above TiO_2 at

870 K being about 10^{-18} mbar [15,16]), and the crystal becomes first yellow and then blue in color. In this case, transport measurements indicate that the crystal becomes an n-type semiconductor, and Paramagnetic Resonance studies show the presence of Ti^{3+} species [4,15]. The oxygen concentration can be restored by heating the reduced crystal in an oxygen atmosphere of about 250 mbar at 870 K for 1 hour, as shown by the color change of the crystal from blue to yellow [15].

In 1952, Cronemeyer [11] found that the blue color of the TiO_2 crystal arises from an optical absorption maximum at 0.73 eV and that further reduction of rutile leads to an opaque crystal. From weight losses and Hall coefficient data he calculated the bulk density of conduction-band electrons to be 10^{20} cm^{-3} in opaque crystals.

From further Infrared Absorption studies [17] Cronemeyer concluded that oxygen vacancies can be considered as doubly ionizable donors (two electrons are trapped at each oxygen vacancy), which are responsible for the conductivity of nonstoichiometric rutile. The existence of several donor levels in the band gap of defective rutile was mainly derived from the temperature dependence of the conductivity and Hall mobility [11,18,19]. Measurements of dielectric constants [20,21], Infared (IR) and Optical Absorption results [11,17] as well as studies of the dependence of the conductivity and Hall mobility on the

degree of reduction of rutile [16] led to the assumption that these donor levels can indeed be assigned to differently ionized bulk oxygen vacancies [22].

In this model, each bulk oxygen vacancy V_O is associated with two Ti^{3+} species ($2Ti^{3+}$ V_O) and can be ionized twice. The corresponding ionization potentials give rise to two different donor levels in the band gap, and were found 0.15 to 0.20 eV and 0.75 to 1.0 eV below the lower conduction-band edge E_C [13].

Ti^{3+} ions in the bulk of rutile may also be described as donors. They are assumed to be located at regular lattice sites [21,23] as well as interstitial sites [24,25]. Electron Spin Resonance (ESR) data [26,27] as well as studies of the internal friction [28,29] support both hypotheses.

Oxygen interstitials were only observed at oxygen partial pressures above 1 mbar [30] and lead to acceptor-type levels in the band gap, and even to p-type conduction at higher oxygen pressures [30].

The oxygen vacancy concentration obtained by a high temperature treatment (see above) with the help of reducing gases (H_2 or H_2O [11,31], CO or CO_2 [25,32]) is "frozen" by quenching down to temperatures below 800 K [33,34]. Although the thermodynamically stable oxygen vacancy concentration was determined to be less than 3.4×10^{12} cm^{-3} at temperatures below 600 K [35,36], no

changes in the bulk stoichiometry are observed below 800 K during the exposure of oxygen. Reversible uptake and removal of oxygen is only observed above 800 K [37].

The diffusion of titanium in the TiO_2 bulk was studied by Carnahan et al. [24], who derived a diffusion activation energy of 1.04 eV from changes in optical absorption.

Haul and Duembgen [38] studied the diffusion of oxygen in TiO_2 by means of gas/solid isotope-exchange experiments with ^{18}O-labelled oxygen. In the temperature range between 980 and 1570 K, they calculated a diffusion activation energy of 2.65 eV and a diffusion coefficient of $2.0 \times 10^{-3} \times \exp(-2.65\ eV/k_BT)\ cm^2/sec$ for oxygen diffusion (see also reference 1).

Many physical properties of rutile TiO_2 such as electrical conductivity, Hall mobility and dielectric constant are highly anisotropic [15] and have been investigated extensively during the last decades.

Different models such as the multiple-band model and the polaron hopping model have been suggested to explain the charge-carrier transport mechanism and thus the conductivity of rutile.

The scattering of electrons at ionic lattice defects and point defects is believed to be the dominant mechanism at temperatures below 50 K [21,39,40], whereas above 80 K

only scattering at acoustic and optical phonons has been considered, in terms of a multiple-band [16,18,40,41] as well as a polaron model [42-44,49].

Becker and Hosler [18] deduced the existence of multiple-band conduction in n-type rutile for temperatures above 40 K from studies of Hall coefficients and electrical conductivities from 2 to 600 K. They calculated the separation between the lowest conduction band and the bottom of the next higher one to be 0.05 eV, and showed that impurity and surface conductivity could be neglected.

Bogomolov and Zhuze [42] performed electrical conductivity and Hall mobility measurements on slightly reduced single-crystal rutile (parallel and perpendicular to the c-axis) in the range of 78 to 700 K. From their low Hall mobility values they concluded that the electrical conductivity of rutile can be described in terms of a hopping model of polarons with large effective masses rather than by a multiple-band model.

In 1968, Goto and Okada [44] presented results obtained from high-frequency conductivity measurements. Their results showed an increase in the bulk conductivity above 100 MHz and a saturation above 24 GHz. The magnitude of the dispersion turned out to be independent of temperature. They attributed the high-frequency conductivity in (reduced) rutile to the hopping conduction of small polarons localized around lattice defects.

Since 1970, both the multiple-band and the polaron model have been accepted as coexisting models [45], according to which free charge carriers are found in conduction bands and electrons trapped at defects are considered as polarons.

Whitehurst et al. [46] as well as Raalte [47] observed an instability in the electrical conductivity of nonstoichiometric ceramic and crystalline titanium dioxide. The conductivity was found to decrease slowly for as much as several hundred hours at constant measuring temperatures lying between 273 and 373 K, following quenching from temperatures between 470 and 670 K. Whitehurst's experimental curves showed that the conductivity varied with time at the measuring temperature according to:

$$\sigma = \sigma_e + B \times \frac{\sigma_0 - \sigma}{t} \qquad (1)$$

where σ, σ_0 and σ_e are, respectively, the conducivities at time t, at t=0 (immediately after quenching) and at equilibrium ($t \rightarrow \infty$). The factor B is a constant during a given isothermal experiment but, in general, depends on σ_0 and σ_e as well as temperature.

Whitehurst et al. interpreted their results in terms of the theory of reaction rates on the assumption that

electrons are trapped out of conduction states into empty traps. They calculated extremely small trapping cross sections of about 2×10^{-27} cm^2 [46].

Extensive studies on bulk Hall mobilities of TiO_2 have been presented in the literature during the last two decades. The Hall mobility μ strongly depends on the crystal temperature T, but does not show a dependence on the charge carrier concentration above 200 K [18,48]. The temperature dependence can be expressed as

$$\mu = a_1 \times T^{-a_2} \qquad (2)$$

where a_1, a_2 are constants [42,48].

In order to describe the mean mobility over a wider temperature range, a more complicated expression is favored:

$$\mu = a_1 \times T^{-a_2} \times [\exp(a_3/T) - a_4] \qquad (3)$$

where a_3 = const. and a_4 = 0 or 1 [16,49].

Due to comparable experimental conditions, the Hall mobilities used in this thesis (see chapter 5) were taken from reference 42, resulting in:

$a_1 = 10^{5.685}$ $cm^2K^{2.5}/Vsec$, $a_2 = 2.5$, $a_3 = a_4 = 0$ (4)

Dielectric constants of rutile TiO_2 were determined experimentally by Parker [50], Dominik et al. [21] as well as Hollander et al. [20]. Measurements were done parallel

and perpendicular to the c-axis, in temperature and frequency ranges from 1.2 to 1060 K and 10^2 to 10^5 Hz, respectively. The dielectric constants ϵ used in this thesis (see chapter 5) were derived from results given in reference 50. The following approximate temperature dependence was obtained in a temperature range from 300 to 420 K:

$$\epsilon \simeq \epsilon_1 x T + \epsilon_2 \qquad (5)$$

where $\epsilon_1 = -0.066\ K^{-1}$ and $\epsilon_2 = 140.7$.

From measurements of electrical and optical properties Frederikse [41] and Breckenridge et al. [16] determined effective masses of conduction band electrons. Using the expressions for the conductivity, Hall coefficient, and thermoelectric power of a nondegenerate electron gas [41], Frederikse calculated the effective electron mass m_{eff} at the bottom of the conduction band to be $25m_e$, where m_e is the rest mass of an electron. The above relationship will be used in the discussion in chapter 5.

Recalculations of Madelung potentials in stoichiometric rutile TiO_2 are reported by Iguchi et al. [51]. They determined Madelung potentials of 29.53 eV at the Ti^{4+} site and -41.20 eV at the O^{2-} site, leading to the value of 141.5 eV for the Madelung energy per TiO_2 "molecule" and also to the value of 4.810 for the Madelung constant.

Soffer [52] as well as von Hippel et al. [4] discovered during Infrared-Spectroscopic experiments that TiO_2 crystals grown by the Verneuil method always contain residual hydrogen, indicated by a narrow double band near 3300 cm^{-1}, the typical OH stretching vibration. Various reactions in hydrogen and oxygen and the effects of reduction on electron mobilization and the Optical Absorption spectrum were studied subsequently. Theoretical studies [53] on the solubility of hydrogen and deuterium, as well as diffusion experiments [54,55] involving hydrogen and deuterium, have also been reported during the last few years. Johnson et al. [54] have measured diffusion coefficients D for hydrogen both parallel and perpendicular to the c-axis; their results are:

$$D_{\parallel} = 1.8 \times 10^{-3} \times \exp(-0.59\ eV/k_B T)\ cm^2/sec \quad \text{and}$$

$$D_{\perp} = 0.38 \times \exp(-1.28\ eV/k_B T)\ cm^2/sec.$$

Surface Structure Including Surface Defects

Titanium dioxide surfaces have been studied by several surface science groups in the past [2,15,56-97]. From the basic science point of view, studies at (110) single-crystal TiO_2 surfaces are of particular interest (geometric model in Figure 2, and reference 80). First, this surface is the thermodynamically most stable surface of TiO_2 [65,79,86,94] and is expected to make possible the study of reversible solid-gas interactions. Secondly, ideal TiO_2 surfaces show no intrinsic surface states in the band gap [65,79,86].

States may, however, be induced by the formation of either point defects of the ideal TiO_2 lattice, such as vacancies or interstitial atoms, or of extrinsic defects associated with foreign atoms [45,57,59,62,63,65,79]. Electronic states in the gap have been associated with the existence of intrinsic, paramagnetic defects [65,79,80], and earlier studies on the defect formation at $TiO_2(110)$ [56,79] indicated that filled band-gap defect surface states correspond to $2Ti^{3+}$ V_{Os} vacancy complexes, although the detailed geometry of those complexes is not precisely known.

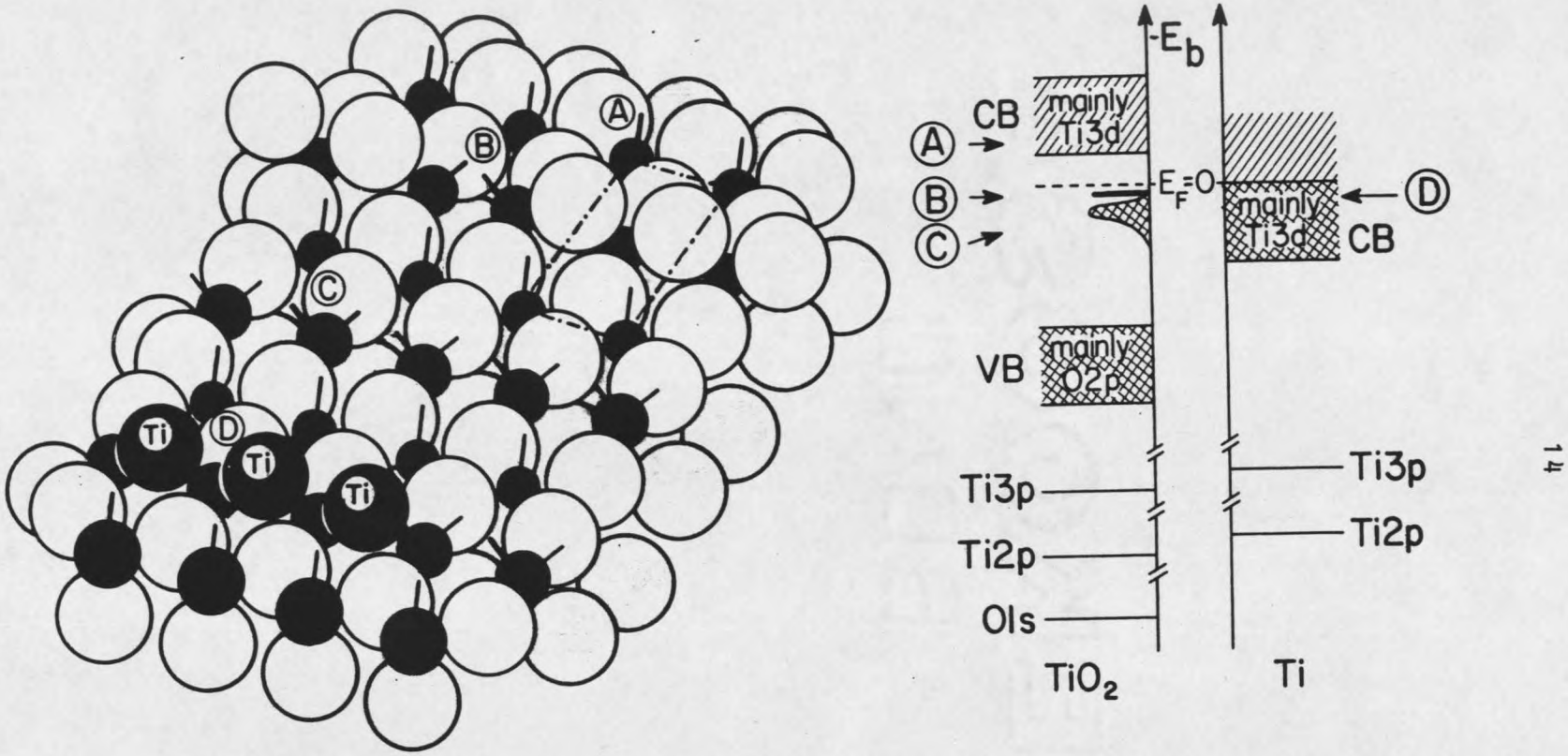

Figure 2. Left: geometric representation of the TiO_2(110) surface with different types of intrinsic defects (see text). White circles represent oxygen, black circles titanium species.
Right: schematic energy diagram for TiO_2 and Ti, indicating the expected energetic positions of the different defects (see reference 80).

The most probable type of surface point defect at TiO_2(110) is shown in Figure 2 (black circles: Ti ions, white circles: O ions) by the missing O ion (labelled B) that bridges two sixfold-coordinated Ti ions. When a bridging O ion is removed, the two neighboring Ti ions become fivefold-coordinated.

However, observations on nearly perfect TiO_2(110) and (100) surfaces [79] show that fivefold coordination may not be sufficient to completely populate band-gap surface states in n-type material resulting in only partially filled donor levels (see reference 79 and chapter 5). For this defect the two Ti ions are very poorly screened from each other, which is somewhat analogous to the situation in bulk Ti_2O_3. This poorly screened pair of Ti ions at the defect site may well share an electron in a similar manner, giving rise to a band-gap surface state. This situation is illustrated in Figure 2, which also presents schematic energy diagrams of TiO_2 as well as Ti. The thick solid line labelled B represents the point-defect (see geometric model) induced donor level in the TiO_2 band gap between the O2p-derived valence band (VB) and the Ti3d-derived conduction band (CB, corresponds to A for the stoichiometric surface). The Fermi level, E_F, indicated by the dashed line, was found to be close to the donor level and changes its relative position to the latter one as a

function of temperature [79]. Thus both partially and completely filled donor levels are possible.

Point defects at TiO_2(110) as indicated by B in Figure 2 can easily be created by high temperature treatments (see references 79-81 and chapter 4) and lead to discrete energy (donor) levels in the band gap. Heavy ion bombardment, however, may result in the formation of line defects accompanied by defect energy bands in the band gap. This phenomenon is illustrated by C in Figure 2 and has been observed during UPS (Ultraviolet Photoemission Spectroscopy) experiments by Henrich et al. [56] as well as Chung et al. [15]. Argon-ion bombardment led to an additional band-gap emission 0.7 eV below the TiO_2 conduction band [56] and was attributed to disorder-induced Ti^{3+}-oxygen-vacancy complexes at the surface.

ELS (Electron Loss Spectroscopy) studies done on ion-bombarded TiO_2(110) surfaces [56] (to be discussed in more detail in chapters 4 and 5) also showed an additional electronic loss feature at a loss energy of 1.9 eV. This feature was assigned to a d-to-d transition involving defect-induced occupied Ti3d states in the band gap as well as empty Ti3d states in the conduction band (see also chapter 5) and has also been detected by Goepel et al. [80,81].

Still further ion bombardment produced ordering of Ti^{3+} pairs into a Ti_2O_3-like surface structure according to

UPS and ELS spectra [56]. The intensities of the defect-induced UPS and ELS features dropped significantly during the exposure to 10^8 L [Langmuir (1L = 1.33×10^{-6} mbar sec)] of oxygen at room temperature as was shown by Henrich et al. [56].

The formation of surface defects at $TiO_2(110)$ apparently results in less positively (compared to the Ti^{4+} ions in the bulk) charged titanium species at the surface due to the occupation of originally empty Ti3d states indicated by B and C in Figure 2.

In a further step of surface chemical reduction, the presence of neutral titanium atoms at the surface will be of interest and is emphasized by big dark circles (labelled D) and a schematic titanium energy diagram in Figure 2. The situation encountered after the deposition of titanium atoms on $TiO_2(110)$ will be discussed extensively in chapters 4 and 5.

Low Energy Electron Diffraction (LEED) studies have been reported, e.g., by Henrich et al. [56], Chung et al. [15], Kao et al. [87] as well as Firment [72]. The stoichiometric $TiO_2(110)$ surface showed a stable (1x1) unreconstructed structure after annealing at 670 K for 15 minutes [15,87] and a (1x2) pattern after an extended annealing at 885 K for 14 hours [87]. A $TiO_2(110)$ surface

sputtered for a dose of $3x10^{15}$ argon ions/cm^2 at an ion energy of 2 KeV exhibited a very diffuse LEED pattern [87].

With the help of UPS measurements, Chung et al. [15] found that the work function increased from 4.6 eV for the TiO_2(110) argon-bombarded surface to 5.5 eV for the well-annealed (110) surface. This result is consistent with that of Henrich et al. [56] reported for the (110) surface. On the other hand, the work function of an initially well-ordered TiO_2(110) surface was unaffected by oxygen-ion bombardment up to $7.2x10^{15}$ ions/cm^2 [15]. Together with the work function measurements and the known values of electron affinity and band gap for TiO_2 (4 and 3 eV respectively), Chung et al. also calculated a surface band bending of 1.7 ± 0.2 eV for both the annealed or oxygen-ion-bombarded (110) surface and 0.9 ± 0.2 eV for the argon-ion-bombarded surface.

Auger Electron Spectroscopy (AES) studies on TiO_2(110) surfaces have been reported, e.g., by Chung et al. [15], Davis et al. [77], Knotek et al. [60] as well as Nishigaki [76]. Chung et al. found an increase in the OKVV/TiLMM ratio from ~1.3 on the argon-ion-bombarded surface to ~1.7 on the annealed TiO_2(110) surface. This ratio turned out to be fairly reproducible over many sputtering-annealing cycles, indicating oxygen deficiency at argon-ion-bombarded surfaces.

During his AES experiments on TiO_2(110) surfaces Nishigaki discovered that the line shape of the Auger transition TiLMV changed upon argon-ion bombardment. He interpreted this phenomenon in terms of Ti^{3+} species at sputtered surfaces, inducing an additional intra-atomic Auger process involving occupied Ti3d states. Similar features have been observed in the course of X-ray-induced Auger Electron Spectroscopy (XAES) studies performed on TiO_2(110) samples by Goepel et al. [80].

The origin of the TiLMV Auger line on stoichiometric and defective TiO_2(110) surfaces is explained in Figure 3 (see also reference 80). A $Ti2p_{3/2}$ (=L) core-hole level is reoccupied by a Ti3p (=M) electron. The de-excitation energy gained in this process causes the emission of a valence-band (V) electron and thus the Auger line TiLMV. Due to the fact that the valence band of TiO_2 is mainly oxygen-derived, the TiLMV Auger transition in TiO_2 is interatomic, involving both titanium and oxygen ions. In the presence of surface defects, however, Ti3d-derived states are found in the band gap (see above) and make possible an additional intra-atomic TiLMV Auger transition (see arrows in Figure 3) involving titanium energy levels only. Owing to the higher cross section for intra-atomic Auger transitions, even very low concentrations of surface defects, i.e. Ti^{3+} ions, cause an additional peak of higher kinetic energy in the TiLMV line.